CLM - M 93
CPG/FRS(72)P.2

HYDRA

A 2-Dimensional Compressible Hydrodynamics Code for Multi-Fluid Calculations

by

M H Hughes

ABSTRACT

HYDRA is a 2-dimensional hydrodynamics code to study the compressible flow of two or more immiscible fluids. This report describes the physical model, the computing technique and the structure and testing of the code.

UKAEA Research Group
Computational Physics Group
Experimental Division B
Culham Laboratory
Abingdon, Berkshire.

June, 1972

CONTENTS

Page

PART I: HYDRODYNAMIC MODEL

1. INTRODUCTION 1

2. PHYSICAL MODEL 2

2.1 The differential equations 2

2.2 Computing method 3

3. FINITE DIFFERENCE METHODS 3

3.1 The mesh 3

3.2 Lax-Wendroff difference equations 4

3.3 Interlaced mesh instabilities 6

3.4 Smoothing shocks 7

3.5 Boundary conditions 7

4. REPRESENTATION OF THE INTERFACE 8

4.1 Motion of the interface 8

4.2 Area weighting 9

4.3 Matching the particle chains 10

4.4 Determination of the fluid composition 10

4.5 Surface tension 12

4.6 Chaining 12

PART II: COMPUTER CODE

5. INTRODUCTION 14

5.1 Program structure 14

5.2 Output from program 17

5.3 Analysers 20

6. PROGRAM TESTING 20

6.1 1D calculations 20

6.2 Kelvin-Helmholtz instability 21

7. FUTURE APPLICATIONS 24

ACKNOWLEDGEMENTS

PART I: HYDRODYNAMIC MODEL

1. INTRODUCTION

Experimental work motivated by several accidents has shown that the sudden contact of hot and cold fluids can sometimes result in violent explosions. Explosive rates of heat transfer can be understood only if one postulates that the interfacial area between the fluids increases rapidly with time as a result of some hydrodynamic instability. Small scale debris observed experimentally shows that hydrodynamic shredding does occur. To improve our understanding of the fluid mechanics involved in these rapid mixing processes a new hydrodynamics code called HYDRA has been written. This report describes the hydrodynamic model, the computing technique and the structure of the code.

HYDRA is designed to study the 2-dimensional compressible flow of immiscible fluids allowing for large amplitude distortions of the interface between them. The code employs an Eulerian finite difference method and to demarcate the fluid boundary a list processing technique originally developed by Roberts and Berk(1) is exploited. Although Eulerian methods have previously been applied to multi-fluid problems, their application has been limited by their tendency to smear out any density discontinuities. This results from the fact that an Eulerian cell containing two fluids is assumed to have the mixture distributed uniformly throughout and when mass fluxes are calculated it is this mixture that is transported. This results in a diffusion that eradicates density discontinuities. HYDRA represents the boundary between the fluids, which may in general comprise several curves, by a chain of straight line segments. Each segment is advected with the local fluid velocity and hence the position of the interface is known at all times.

The remainder of part 1 of this report describes in detail the physical model and numerical methods incorporated in the code; part 2 describes the program structure, testing and application.

2. PHYSICAL MODEL

2.1 The differential equations

The equations representing conservation of mass, momentum and energy in a compressible fluid can be written in the form

$$\frac{\partial \rho}{\partial t} = - \operatorname{div}(\rho \underline{v}) \tag{1}$$

$$\frac{\partial}{\partial t} (\rho v_i) = \frac{\partial P_{ij}}{\partial x_j} \tag{2}$$

$$\frac{\partial E}{\partial t} = - \operatorname{div}(g) \tag{3}$$

where the density is denoted by ρ and the velocity by $\underline{v}$. The total momentum tensor is

$$P_{ij} = p\delta_{ij} + \rho\, v_i\, v_j - V_{ij} \tag{4}$$

and the viscous stress tensor is

$$V_{ij} = \mu\left(\frac{\partial v_i}{\partial x_j} + \frac{\partial v_j}{\partial x_i}\right) + \lambda\, \frac{\partial v_i}{\partial x_i} \tag{5}$$

with μ the coefficient of dynamic viscosity and λ the coefficient of bulk viscosity. The total energy is

$$E = \tfrac{1}{2}\, \rho\, v^2 + \rho I \tag{6}$$

and the energy flux vector is

$$\underline{g} = \underline{v}(p+E) - V_{ij}\, v_i\, \underset{\sim}{e}_j - K \operatorname{grad} T \tag{7}$$

where I is the specific internal energy, T is the temperature, K is the thermal conductivity and $\underset{\sim}{e}$ is a unit vector. The above equations together with an equation of state relating the pressure p and temperature T to the specific internal energy I and the density ρ are sufficient to determine the hydrodynamic flow subject to some boundary conditions.

Equations (1) - (3) are readily solved by the Lax-Wendroff difference scheme(2) where exact conservation of mass, momentum and energy can be guaranteed. The difference scheme is discussed fully in section 3.2.

When there are two fluids present provision must be made for discontinuous changes in ρ, μ and K at the interface. Moreover, there may also be a surface tension force at the interface between the fluids.

2.2 Computing Method

The computing method subdivides the material region into a finite mesh of cells. The fluid boundary is represented on this mesh by a chain of straightline segments; the junction of two segments is referred to as a node. The solution of equations (1) - (3) is obtained at each mesh point using a finite difference method and the local fluid velocity $\underline{v}_i$ at the location of each node i is obtained from the mesh by interpolation; each node is then advected with the local velocity $\underline{v}_i$ according to

$$\frac{dx_i}{dt} = \underline{v}_i \quad . \tag{8}$$

From the position of the interface, the fluid composition of each Eulerian cell can be found and hence the equation of state, the thermal conductivity coefficient and the viscosity coefficient which are to be inserted in the fluid equations of motion. Also, since the orientation of the interface is known it is possible, in principle, to include the effect of surface tension at the fluid boundary.

As the fluid motion develops the interface, in general, becomes longer. To maintain adequate resolution a list processing technique(1) is used to insert and remove nodes if segments along the interface stretch or contract too much during the course of a calculation.

3. FINITE DIFFERENCE METHODS

3.1 The mesh

The material region is divided into a finite mesh of cells in the manner illustrated in Fig.1. The solid lines represent the boundaries of the physical region and the surrounding points, called guard points, are employed to facilitate the application of some boundary conditions (§3.5). Values at the guard points are determined from some symmetry condition. This enables the difference equations to be used right up to the physical boundary, so simplifying and speeding up the calculation.

The points represented by crosses and those represented by circles in Fig.1 are defined at different times. The reason for this will become apparent in the next section.

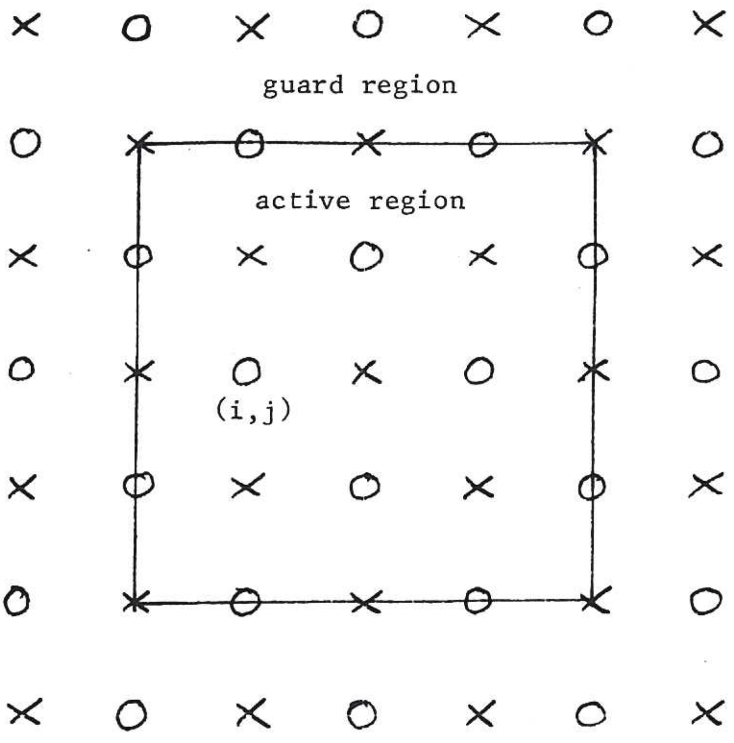

Fig. 1

3.2 Lax-Wendroff difference equations

In two space dimensions, the conservation equations (1) - (3) can be written in the vector form

$$\frac{\partial U}{\partial t} + \frac{\partial}{\partial x} F(U) + \frac{\partial}{\partial y} G(U) = 0 \tag{9}$$

where

$$U = \begin{bmatrix} \rho \\ m \\ n \\ E \end{bmatrix} , \quad F(U) = \begin{bmatrix} m \\ m^2/\rho+p \\ mn/\rho \\ (E+p)m/\rho \end{bmatrix} , \quad G(U) = \begin{bmatrix} n \\ mn/\rho \\ n^2/\rho+p \\ (E+p)n/\rho \end{bmatrix}$$

in which

ρ is the mass per unit volume

u is the horizontal velocity component

v is the vertical velocity component

m is ρu

n is ρv

E is total energy per unit volume

p is pressure.

HYDRA solves equation (9) using a two-step Lax Wendroff procedure with second order accuracy(2). Referring to Fig.1, the circle points are defined at even times $2n\Delta t$ and the cross points at odd times $(2n + 1)\ \Delta t$. The first step entails calculating auxiliary variables at the cross points using the first order scheme

$$U^{(2n+1)\Delta t}_{i+1,j} = \tfrac{1}{4}\left(U^{2n\Delta t}_{i+2,j} + U^{2n\Delta t}_{i,j} + U^{2n\Delta t}_{i+1,j+1} + U^{2n\Delta t}_{i+1,j-1}\right)$$

$$- \frac{\Delta t}{2\Delta x}\left(F^{2n\Delta t}_{i+2,j} - F^{2n\Delta t}_{i,j}\right) - \frac{\Delta t}{2\Delta y}\left(G^{2n\Delta t}_{i+1,j+1} - G^{2n\Delta t}_{i+1,j-1}\right) . \tag{10}$$

The auxiliary variables are used to construct fluxes at the intermediate time which are then used to advance the main variables from t^{2n} to t^{2n+2} as follows:

$$U^{(2n+2)\Delta t}_{i,j} = U^{2n\Delta t}_{i,j} - \frac{\Delta t}{\Delta x}\left(F^{(2n+1)\Delta t}_{i+1,j} - F^{(2n+1)\Delta t}_{i-1,j}\right)$$

$$- \frac{\Delta t}{\Delta y}\left(G^{(2n+1)\Delta t}_{i,j+1} - G^{(2n+1)t}_{i,j-1}\right) . \tag{11}$$

The scheme is stable[2] if the timestep Δt is chosen to satisfy a Courant-Levy-Friedrichs condition

$$\Delta t < \frac{\Delta}{\sqrt{2}\,(|\underset{\sim}{u}| + c)}$$

where Δ is the space-step, c is the local adiabatic sound speed and $\underset{\sim}{u}$ is the fluid velocity.

The diffusion terms which appear in the momentum and energy equations are included as follows.

(a) Heat conduction

When constructing the auxiliary variables at the cross points, heat conduction is ignored. The diffusion fluxes are calculated at the intermediate time level and used during the second half of the cycle when the physical points are advanced. Thus, the conductivity coefficient, which can be a function of temperature, is calculated at the points N, S, W, E (Fig.2) and grad T is calculated at these points using FN, FS, FW and FE. This first order method for the heat conduction is justified if the diffusion is sufficiently small.

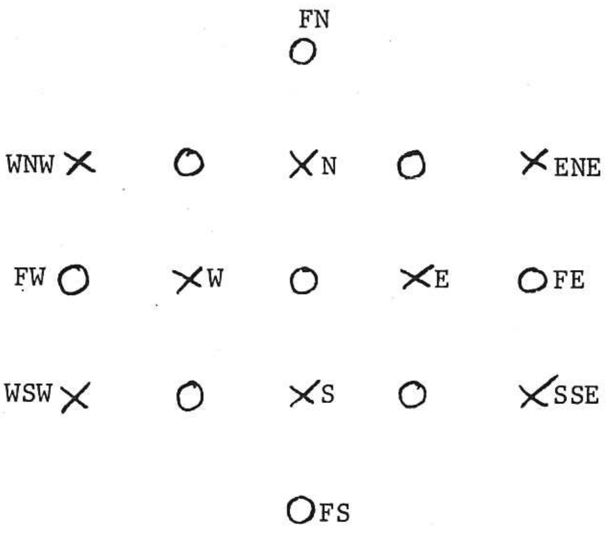

Fig. 2

(b) Viscosity

Viscosity is also ignored during the auxiliary step and included during the main step but this time the derivatives are properly time-centred. The terms $\partial v_i/\partial x_j$ are calculated using the points N, ENE, ESE, S .... etc. and the viscosity coefficient, which is also a function of temperature, is calculated at N, S, W and E.

3.3 Interlaced mesh instabilities

The grid described previously has two interlaced meshes comprising points like those labelled 1 and those labelled 2 in Fig.3. These points are not linked together advectively and the scheme employed for the diffusion terms does not provide any coupling. Thus, some *ad hoc* filtering must be applied periodically to remove unwanted computational modes[3] which may otherwise grow catastrophically. A tentative scheme currently used by HYDRA constructs the following average at each physical point

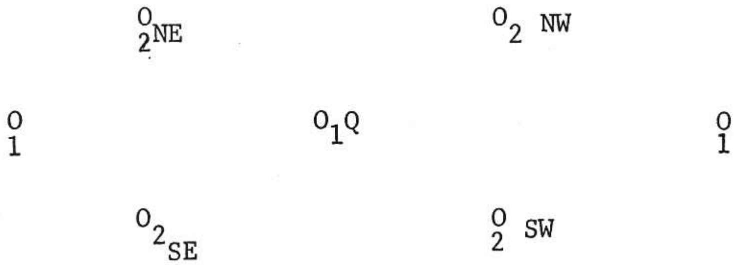

Fig.3

$$\bar{U}(Q) = (U(Q) + \tfrac{1}{4}(U(NE) + U(NW) + U(SE) + U(SW)))/ 2 \; .$$

3.4 Smoothing shocks

It is well known that the dispersive nature of the Lax-Wendroff difference scheme leads to non-linear oscillations in the region of a shock(4)(5). To remove this effect a short wavelength diffusion is added which preserves the high order accuracy of the calculation(4). At the completion of each main step of the Lax-Wendroff calculation, the dependent variables are replaced by new values as follows:

(a) each line of the mesh is scanned replacing $U^{n+1}_{j,k}$ by $U^{1\,n+1}_{j,k}$ where

$$U^{1\,n+1} = U^{n+1}_{j,k} + c\,\Delta^1 \left[\left| \Delta^1 Vx_{j+1,k} \frac{\Delta t}{\Delta} \right| . \Delta^1 U^{n+1}_{j+1,k} \right] ;$$

b) each row is scanned replacing $U^{1\,n+1}_{j,k}$ by $U^{11\,n+1}_{j,k}$ where

$$U^{11\,n+1}_{j,k} = U^{1\,n+1}_{j,k} + c\,\Delta^{11} \left[\left| \Delta^{11} Vy_{j,k+1} \frac{\Delta t}{\Delta} \right| . \Delta^{11} U^{1\,n+1}_{j,k+1} \right] ,$$

$$\Delta^1 f_{j,k} = f_{j,k} - f_{j-1,k}$$

$$\Delta^{11} f_{j,k} = f_{j,k} - f_{j,k-1}$$

and c is a constant. The application of this scheme affects only short wavelengths ($\lambda \sim$ mesh spacing, Δ) and leaves longer wavelengths unperturbed since the diffusion coefficient is a variable such as to be finite only for $\lambda \lesssim \Delta$.

3.5 Boundary conditions

For any specific problem it is necessary to supply an appropriate set of boundary conditions. The present version of HYDRA provides for periodic boundary conditions or rigid free-slip walls in either direction. However, there is provision in the code for defining more complicated ad hoc situations, such as internal obstacles, if required.

The boundary conditions in the y-direction will be discussed below; the conditions in the x-direction are exactly analagous. The indices i,j refer to a point on the bottom boundary of the mesh. Thus, if the boundary conditions in the y-direction are periodic we have

$$U_{i,\,j\,+\,NY} = U_{i,\,j} \;;\; U_{i,\,j\,-\,1} = U_{i,\,j\,+\,NY\,-\,1}$$

where U represents any variable and NY is the number of mesh intervals in the y-direction.

If the boundary is rigid, the basic condition is that the normal velocity component vanishes. Moreover, we assume that the dimensions, of viscous boundary layers are small compared with the dimensions of a mesh cell (free-slip condition). In this case the tangential velocity at a guard point (Fig.1) is simply the value at its image point in the active region. The normal velocity at a guard point is the negative of the image value; this makes the average of the exterior and interior normal components zero, consistent with the vanishing of the normal component at the wall.

It is also necessary to apply a boundary condition at the interface between the two fluids. Thus, it is assumed that the pressure is continuous across the boundary. Knowing the mean density of a cell containing the interface, the fractions of either fluid in the cell (§4.4) and a relationship between p and ρ it is then possible to determine the density of either fluid in the cell and hence the pressure.

The preceding sections have discussed the physical model and the finite difference representation of the system. It was indicated that a knowledge of the position of the interface and hence the fluid composition of each Eulerian cell is an essential part of the calculation. The following sections describe the treatment of the interface between the fluids.

4. REPRESENTATION OF THE INTERFACE

To demarcate the position of the interface at all times, each curve is represented by a chain of straight line segments where each node is regarded as a Lagrangian "particle" which is advected with the fluid.

4.1 Motion of the interface

The motion of each node i is followed according to

$$\frac{d\underline{\underline{x}}i}{dt} = \underline{V}_i$$

where V_i , the velocity at the location of the node, is obtained from the mesh by interpolation. With the mesh velocities defined at integral times and the position of the nodes defined at half-integral times it is almost possible to use a time-centred leapfrog scheme to advance the interface :

$$\underset{\sim}{x}^i(t+\frac{\Delta t}{2}) = \underset{\sim}{x}^i(t-\frac{\Delta t}{2}) + \underset{\sim}{V}^i(t)\,\Delta t$$

where $\underset{\sim}{x}^i$ is the position of node i and $\underset{\sim}{V}^i$ is the velocity at the location of the node. However, the velocity $\underset{\sim}{V}_i$ (t) cannot be obtained by interpolation from the mesh until the positions at time t are known. To circumvent this difficulty, HYDRA employs two sets of nodes; auxiliary nodes whose positions are known at auxiliary (half-integral) times and main nodes whose positions are known at integral times.

After the first step of the two-step Lax-Wendroff calculation, the <u>auxiliary</u> nodes are moved from the time level $t - \Delta t/2$ to level $t + \Delta t/2$ using the <u>main</u> chain to evaluate the velocity at time t. Knowing the position of the interface at time $t + \Delta t/2$, the pressure distribution at this time can be found and the second step of the Lax-Wendroff calculation completed. At this stage, the <u>main</u> nodes are moved from t to to + Δt using the auxiliary chain to find the velocity $\underset{\sim}{V}_i$ at $t + \Delta t/2$. We can then calculate the pressure distribution at $t + \Delta t$ in order to proceed to the next cycle.

4.2 Area weighting

The fluid velocity at the location of a node n (Fig.4) is obtained from the mesh by interpolation. Referring to Fig.4 the area weighting[6] scheme is as follows:

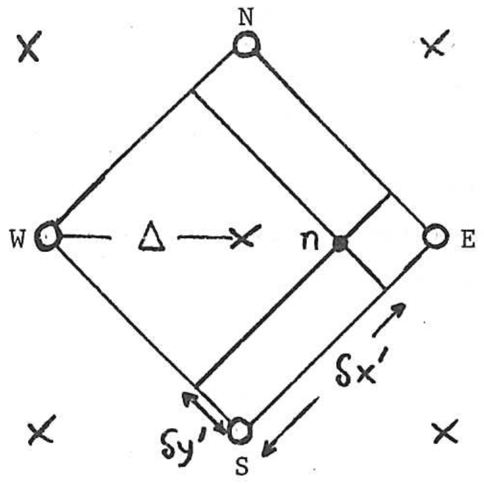

Fig. 4

$$VX_n = \delta y^1 \delta x^1 VX(N) + (\ell-\delta x)(\ell-\delta y^1)VX(S) + (\ell-\delta x^1)\delta y^1 VX(W) + \delta x^1(\ell-\delta y^1)VX(E)$$

where VX_n is the x-component of velocity at the location of the node, N, S, W, E are the four nearest defined points, δx^1, δy^1 are the coordinates of n relative to point S, and $\ell = \Delta\sqrt{2}$ is the length of the square. The y-component of velocity is calculated in an identical fashion.

4.3 Matching the particle chains

As explained above, the HYDRA model employs two associated curves, main and auxiliary, to represent each physical interface curve. Any small misalignment of the two curves can lead to spurious motions$^{(1)}$ and to prevent this from becoming too serious we stop the calculation periodically and re-adjust the positions of the nodes. Currently, the simple first order scheme described below is used.

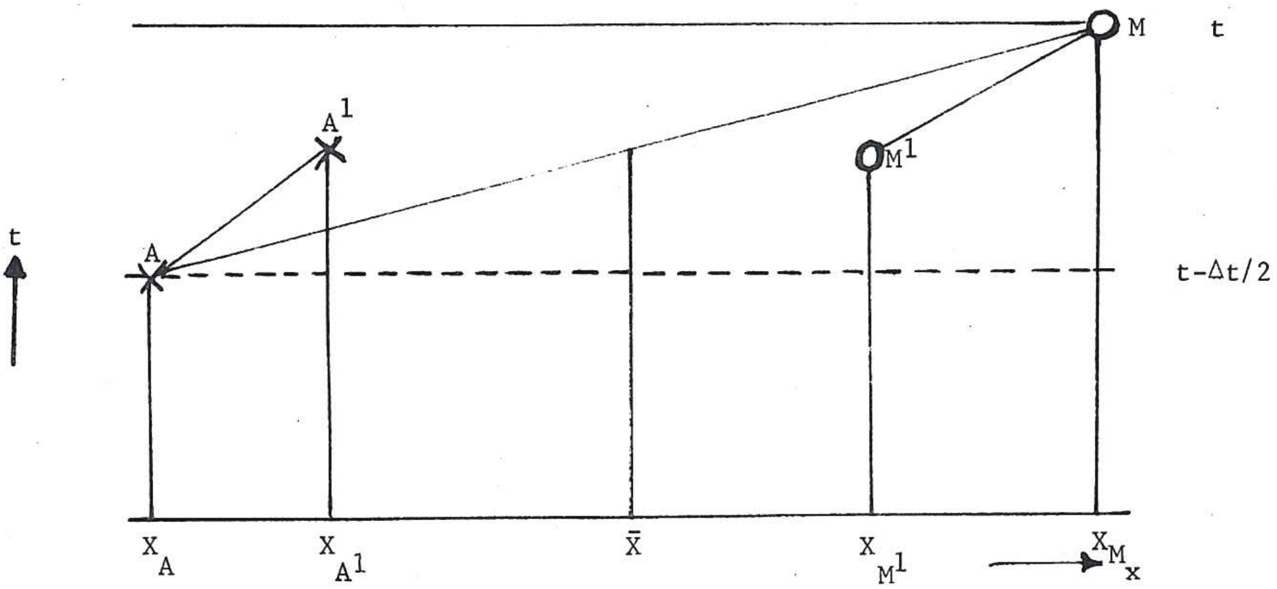

Fig. 5

The calculation is stopped at time t and, using the area weighting scheme described previously, the velocity at time t is used to estimate the position of the node at time t - Δt/4; similarly the position of the corresponding auxiliary node at t - Δt/4 is estimated using the velocity field defined at t - Δt/2 (which are still available in the computer store). Due to misalignment of the chains, the new positions A^1 and M^1 of the nodes (Fig.5) will not in general coincide. The average

$$\bar{X} = (X_A + X_M)/2$$

is calculated and the positions of the main and auxiliary nodes adjusted to

$$X_A^* = X_A + (\bar{X} - X_A1)$$

$$X_M^* = X_M - (\bar{X} - X_M1) .$$

4.4 Determination of the fluid composition within each cell

Given a <u>directed</u> interface as in Fig.6 (which may comprise any number of disjoint parts) it is possible to find the fraction of each material which lies in each Eulerian cell so that the appropriate equation of state and transport coefficients can be determined. This proceeds in the following way:

(a) Scan over each directed segment (i,i+1).

(b) If the end-points lie in different cells, break it into sub-segments, each of which lie entirely in one cell.

(c) Find the cell in which each sub-segment lies (see Fig.6).

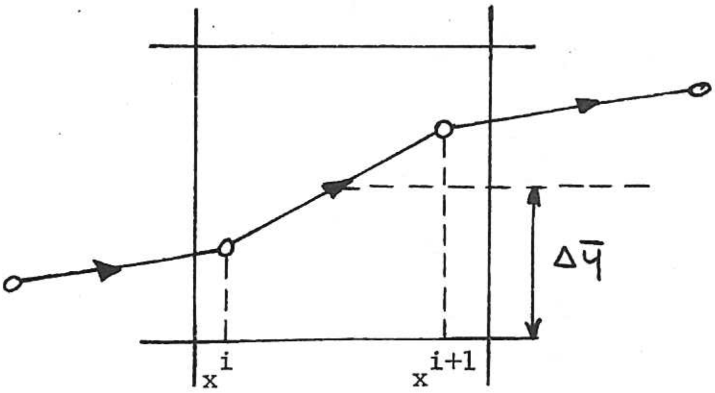

Fig. 6

(d) In one 2D array A, accumulate the signed quantity

$$(x^{i+1} - x^i)\ \Delta\bar{y}$$

This gives the area of material 2 which the sub-segment contributes to this particular cell.

(e) In a second 2D array B, accumulate the signed quantity

$$(x^{i+1} - x^i)$$

This gives the effect of the segment on cells lower down in the same column.

When the scan over segments is complete, an integration in the form

$$A + \int_{ymax}^{y} B\, dy$$

determines the amount of material 2 in each cell. This can be seen pictorially from Fig.7 . The sum of all segments $P_1 \rightarrow P_2$ contributes an area a to cell I (via A), and an area α to all lower cells (via B). The sum of all segments $P_3 \rightarrow P_4$ contributes an area b to I, and β to all lower cells. The sum of all segments $P_2 \rightarrow P_3$ does not contribute at all to I, but contributes c to II (via A), and γ to III and lower cells (via B). Thus the total area of fluid 2 in cell I is (a+b), in cell II it is (α+c+β), while cell III is completely filled with fluid 2 as shown in the diagram.

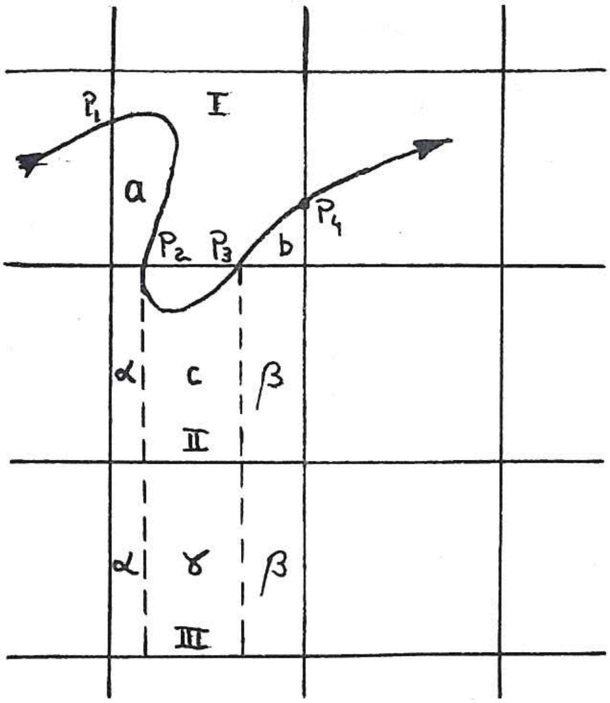

Fig.7

4.5 Surface tension

Although not incorporated in HYDRA at present, surface tension can, in principle, be included by treating each segment as an elastic spring. If the segment lies wholly within a cell then it does not exert a force on that cell. On the other hand, if the segment crosses a cell boundary there is a net surface tension force σ acting on the cell which perturbs the momentum of that cell an amount $\sigma\Delta t$ where Δt is the timestep; this results in a velocity perturbation $\sigma\Delta t/\rho$. The dependence of surface tension on temperature can be included by evaluating the temperature at the point of intersection of the segment and the cell boundary by area weighting.

4.6 Chaining

As the fluid motion develops, the interface becomes contorted and, in general, longer. To take account of this a variable number of points is used to describe the interface, each point (node) being chained[1] to the next in the computer store. Each node is numbered and their locations on the mesh are stored in the computer memory in random locations

$$\ell_B , \ell_1 , \ell_2 \ldots\ldots \ell_n , \ell_E .$$

The storage location of the node ℓ' which follows the node ℓ is obtained from a successor function , NEXT , where

$$\ell^1 = \mathrm{NEXT}\ (\ell)\ ;$$

the serial number of the first node, labelled B, is obtained from another array b_j . The interface curves may be closed or periodic in which case

$$\mathrm{NEXT}(\ell_E) = \ell_B$$

or the curves may be open. All unused nodes are linked together to form a free list whose first element is b_o .

To maintain adequate resolution the length δs of each segment is examined at intervals and if any segment is found to be too long it is broken in half and a new node inserted at the centre giving two segments of length $\delta s/2$. A point δ can be inserted between α and β by writing

$$\ell_\delta = b_o\ ,\ b_o = \mathrm{NEXT}(b_o),\ n_o = n_o - 1,\ n_j = n_j + 1$$

(remove the first point of the free list and assign it to curve j) and

$$\mathrm{NEXT}(\ell_\alpha) = \ell_\delta\ ,\ \mathrm{NEXT}(\ell_\delta) = \ell_\beta$$

(insert the new location between ℓ_α and ℓ_β in the chain).

Similarly if any pair of adjacent segments becomes too short, the central node can be removed in order to save storage space. A point β lying between α and δ can be removed and the location added to the free list by writing

$$\mathrm{NEXT}(\ell_\alpha) = \ell_\delta\ ,\ n_j = n_j - 1,\ \mathrm{NEXT}(\ell_e) = \ell_\beta\ ,$$

$$\ell_e = \ell_\beta\ ,\ n_o = n_o + 1$$

where ℓ_e is defined to be the last free node.

PART II: THE COMPUTER CODE

5. INTRODUCTION

HYDRA is a member of a class of computer codes referred to at Culham as OLYMPUS. The code is designed and constructed around the control package CRONUS[7] and is written to a set of standard rules. The program is written entirely in ISO FORTRAN and can readily be transferred from one computer system to another. However, the code is designed in such a way that sections with high execution frequency can eventually be replaced by faster versions written in Assembler Language on one particular system. Considerable effort has been spent in ensuring that the code is intelligible and that *ad hoc* changes can readily be incorporated. The following sections discuss the general structure of the code, the output generated and various utility routines and analyser programs which are available.

5.1 Program structure

HYDRA is based on a standard framework called CRONUS for solving time-dependent problems. A block diagram of the main control subroutine COTROL is shown in Fig.8. This subroutine controls the calculation and initiates a number of actions which must be carried out before a run is started or re-started. To initiate a run COTROL calls subroutines to :

1. clear COMMON storage (CLEAR);
2. fetch re-start record if appropriate (RESUME);
3. label the run (LABEL);
4. set default values of variables where possible (PRESET);
5. define housekeeping data for a specific run e.g. number of timesteps etc. (DATA).
6. constant auxiliary variables from data obtained through subroutine DATA (AUXVAL);
7. set up initial conditions (INITAL);
8. any further work required before the calculation can start (START).

Fig. 9 is a block diagram of subroutine INITAL and illustrates how complex initial conditions are set up. Having first of all set up the particle lists (in FLIST) a user supplied routine SOURCE is called where the configuration of the interface is defined; HYDRA supplies a number of utility routines for this purpose. The fluid composition is then calculated by COMPSN and routine SETUPV is called which initiates a scan of the mesh. SOURCE is again called at each mesh point and the mesh variables are defined.

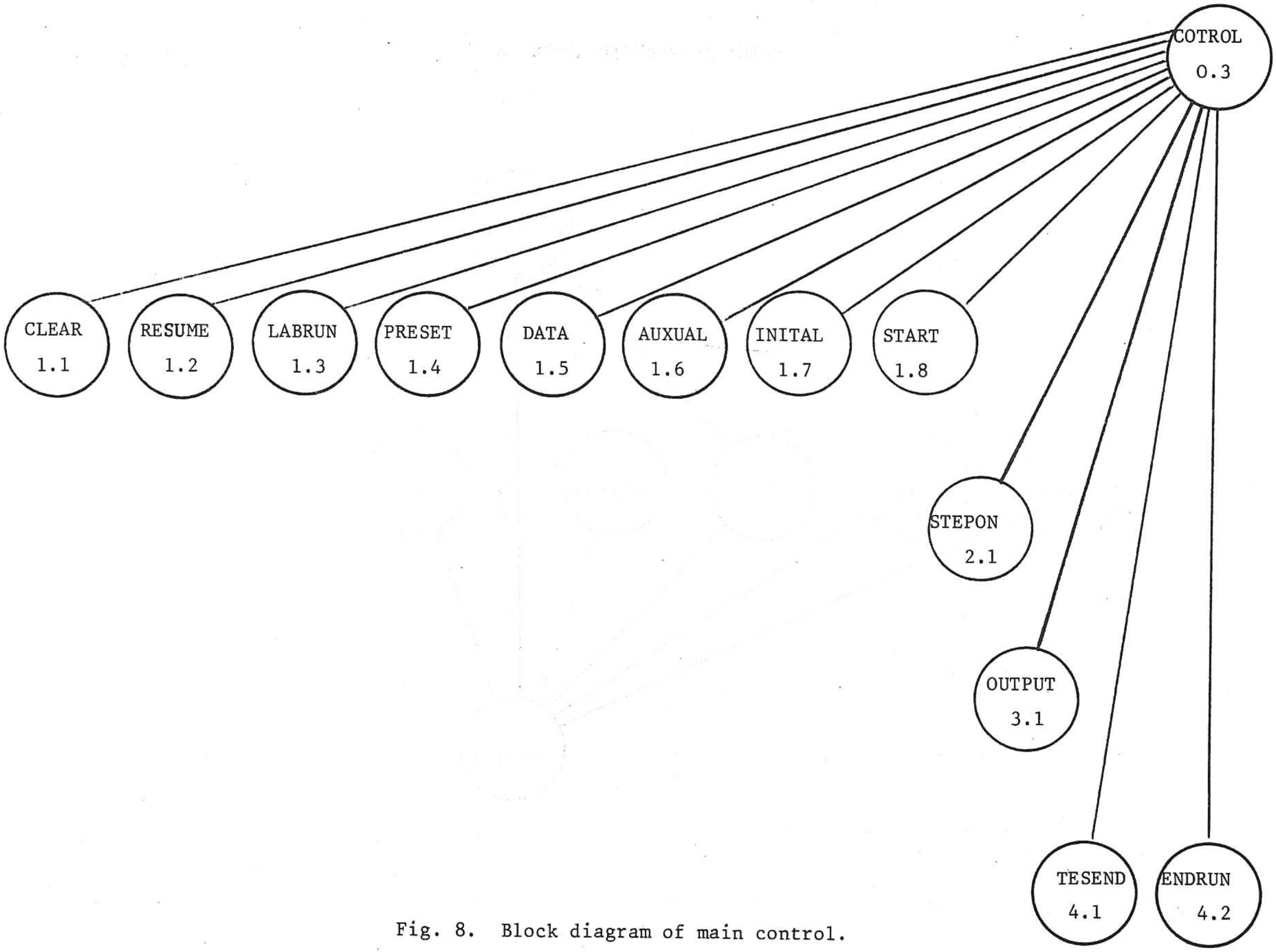

Fig. 8. Block diagram of main control.

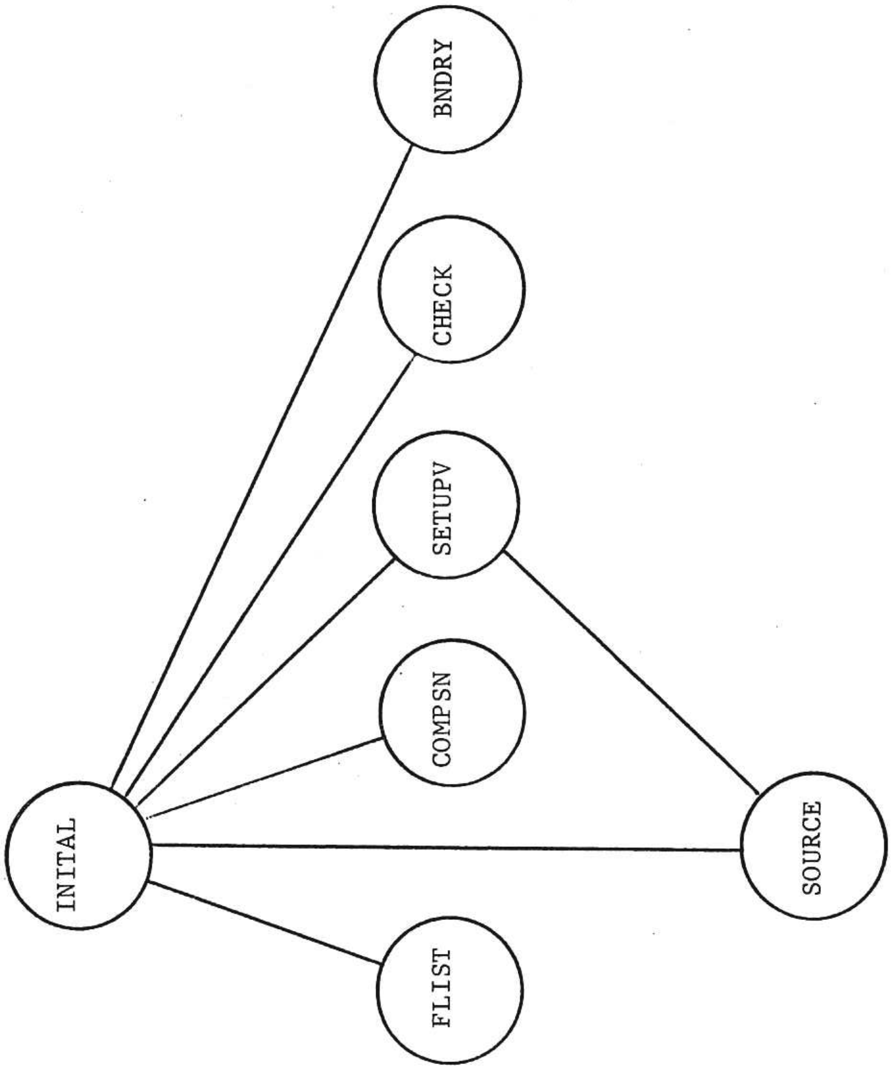

Fig. 9 Block diagram of INITAL

The user, therefore, need not concern himself with the logic of scanning the mesh and setting up storage indices. Finally, a subroutine called CHECK ensures that the initial conditions have been properly defined and BNDRY sets the guard points according to the boundary conditions.

The general principle of separating the logic from the physics is similarly applied in the main calculation loop; fig. 10 is a block diagram of the inner loop and Table 1 gives a list of the subroutines involved and an indication of their function. This makes it very easy for the user to define any equations of state, thermal conductivities and viscosity coefficients (which can be functions of temperature).

If an experienced user wishes to change any part of the program while retaining the basic structure a dummy subroutine EXPERT is called frequently from various parts of the program. By including his own version of EXPERT, the user is able to carry out ad hoc changes e.g. construct internal boundaries.

5.2 Output from program

A typical production run of HYDRA involves very large amounts of data. For example, there are typically 10^4 mesh points with 11 variables defined at each point and possibly several thousand nodes. Such an enormous amount of information can only be digested in graphical form though it is also necessary to print sample diagnostics periodically to ensure that the calculation is proceeding correctly. In-line graphics include plots of the nodes and vector plots of the velocity field; off-line output includes contour plots and isometric projections of the total energy, pressure, density and temperature. In addition, a diagnostic routine PROBE will sample any mesh variable at any point on the mesh (by area weighting) and utility output routines are available for plotting this information.

As the calculation proceeds, checkpoint records are dumped periodically in a ledger file. Each record contains sufficient information to restart a run from that point either using HYDRA or some other analyser program.

A checkpoint record comprises the whole of COMMON. Writing such a record is inherently a slow process and since each record is large only rather few can be contained on a single magnetic tape; checkpoint records are therefore written rather infrequently (say every 20 timesteps). Thus, a second analysis file is written which contains only some control information and selected variables. These records can be written at every timestep if necessary and are designed for use with analyser programs described below.

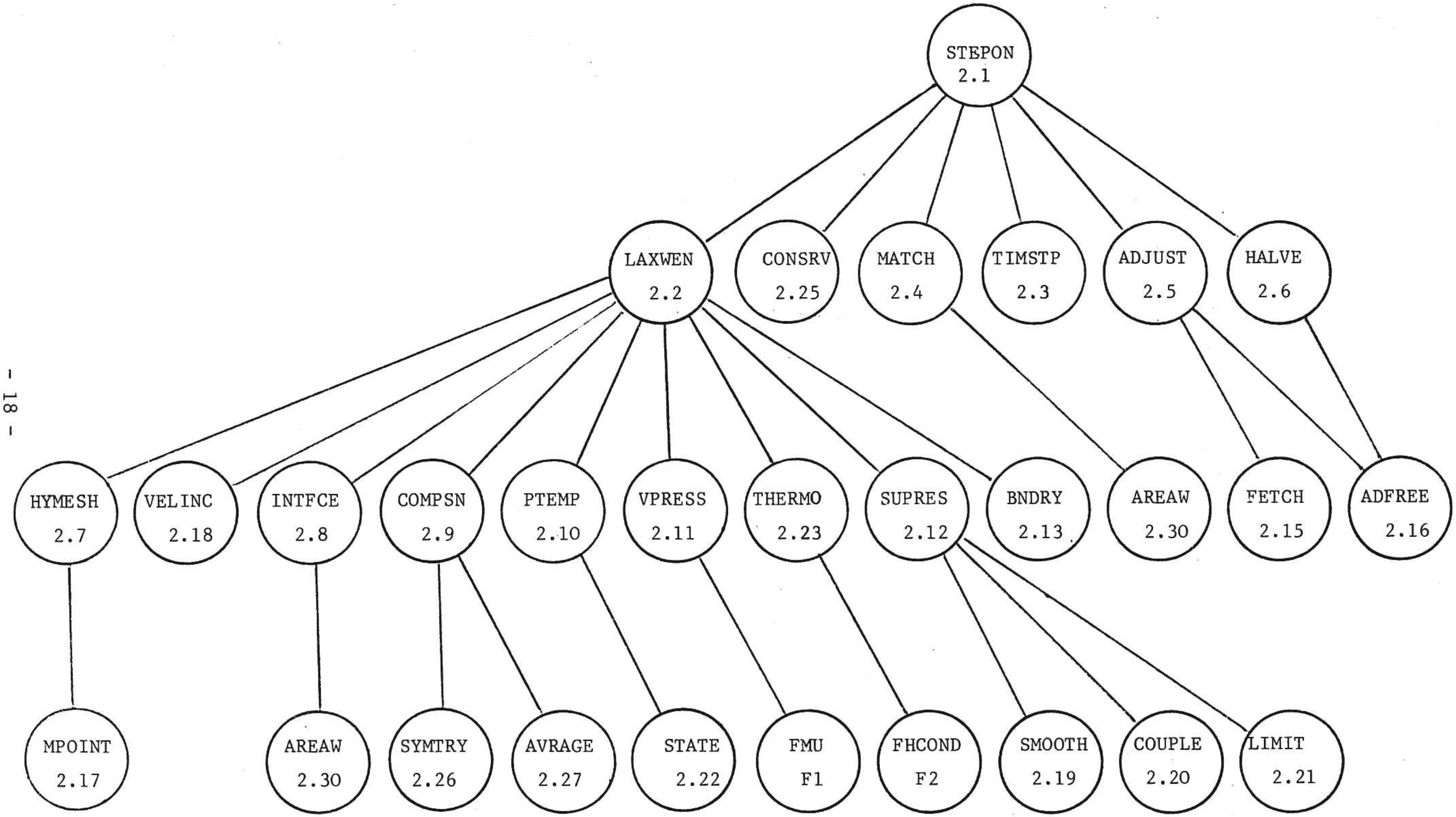

Fig. 10 Block diagram of inner loop.

SUBROUTINE	FUNCTION	LABEL
STEPON	SUPERVISE THE CALCULATION	2.1
LAXWEN	BOTH STAGES OF LAX-WENDROFF CALCULATION	2.2
TIMSTP	FIND NEXT VALUE OF TIMESTEP DT	2.3
MATCH	KEEP MAIN AND AUXILIARY NODES IN STEP	2.4
ADJUST	INSERT OR REMOVE NODES	2.5
HALVE	REMOVE EVERY ALTERNATE NODE	2.6
HYMESH	SCAN OVER THE HYDRODYNAMIC MESH	2.7
INTFCE	ADVANCE POSITION OF INTERFACE	2.8
COMPSN	EVALUATE THE FLUID FRACTIONS IN EACH CELL	2.9
PTEMP	FIND THERMAL PRESSURES AND TEMPERATURES	2.10
VPRESS	FIND THE VISCOUS STRESS TENSOR	2.11
SUPRES	SUPRESS COMPUTATIONAL EFFECTS	2.12
BNDRY	APPLY BOUNDARY CONDITIONS	2.13
FETCH	FETCH NODE FROM FREE LIST	2.15
ADFREE	RETURN NODE TO FREE LIST	2.16
MPOINT	RECALCULATE THERMODYNAMIC VARIABLES AT POINT	2.17
VELINC	VELOCITY INCREMENT DUE TO SURFACE TENSION	2.18
SMOOTH	ARTIFICIAL SMOOTHING OF SHOCKS	2.19
COUPLE	COUPLE THE MESHES	2.20
LIMIT	LIMIT THE VARIATIONS	2.21
STATE	EQUATIONS OF STATE	2.22
THERMO	CALCULATE THERMOMETRIC CONDUCTIVITY	2.23
CONSRV	CALCULATE CONSERVED QUANTITIES	2.25
SYMTRY	APPLY SYMMETRY CONDITION AT BOUNDARIES	2.26
AVRAGE	FINDS AVERAGE ON A LAX-WENDROFF MESH	2.27
AREAW	INTERPOLATE TO FIND LOCAL VELOCITY	2.30
FMU	KINEMATIC VISCOSITY COEFFICIENT	F1
FHCOND	THERMAL CONDUCTIVITY COEFFICIENT	F2

TABLE 1

5.3 Analyser programs

A number of programs are currently available to analyse, off-line, data generated by HYDRA. These include:

1. CONTOR - plot contours of pressure, density, total energy and temperature;
2. SEK3 - a package written by P Dewar for plotting isometric projections;
3. MODANA - a package developed by J P Christiansen which examines the modes excited at the interface and produces phase-plane diagrams and growth rates;
4. MARKER - a marker - and - cell calculation which shows the fluid motion by moving marker particles in the velocity field generated by HYDRA.

6. PROGRAM TESTING

During development of the program each subroutine or set of subroutines having a well defined task to perform was checked in a "test-bed" program. Test-beds were carefully planned in advance and designed to test as many paths through a routine as could be foreseen. A test program comprised a simple set of initial conditions defined on a small mesh (e.g. NX = NY = 4) and only a few nodes when correct results could easily be obtained by hand. In this way it was demonstrated that each section of the program functioned in the way it was intended. Once a routine had passed its acceptance test it was included in the program. Subsequently the assembled program was checked in a similar fashion.

Having completed the test-bed checks a number of simple physical tests were carried out to establish confidence in the code. These are described below.

6.1 1-D calculations

(a) Shock waves

To test the fluid calculation and the smoothing of shock waves, a single fluid was given a uniform velocity (of the order of the sound speed) in the x - direction and brought to rest by a rigid wall; this problem is readily solved analytically. In the absence of any physical diffusion the computed shock speed was in good agreement (better than 1%) with the analytical value when the numerical smoothing was sufficient to eliminate short wavelength "ringing" near the shock front. In the absence of any smoothing energy absorbed by the oscillations reduced the speed of the shock front by ∿ 5%

(b) Heat conduction

To test the conductivity calculation a plane interface was defined at $y = y_o$. The region $y > y_o$ was of one substance whose density, conductivity coefficient and diffusivity were Q_1, κ_1, κ_1 and $y < y_o$ was another substance Q_2, K_2, κ_2. Initially the temperature distribution was

$$T = \text{constant } T_1 \qquad y > y_o$$

$$T = \text{constant } T_2 \qquad y < 0$$

and the pressure was everywhere P_o. The solution of this problem with K_1 and K_2 constant is known and the agreement between the numerical and analytic solutions was satisfactory.

6.2 Kelvin-Helmholtz instability.

The linear stability of the interface between two compressible fluids in relative motion has been considered by several authors(8)(9)(10). We consider two compressible fluids in a steady state separated by a plane interface at $y = y_o$; the fluids have translational velocities parallel to the interface. The stability of the interface is considered when it is subjected to a small perturbation. It is necessary to distinguish two cases depending whether the steady flow is subsonic or supersonic in a coordinate system in which the interface wave is at rest.

(a) Subsonic flow

When the flow is subsonic it can be shown that the interface is unstable. The growth rate of the instability, apart from a small correction for the compressibility, is essentially that for incompressible flow.

This calculation was set up numerically with periodic boundary conditions in the x-direction and fixed boundaries in the y-direction. The steady state flow speed U parallel to the interface was $\pm \frac{1}{2}$ (sound speed). Further, to obtain physically meaningful results it was necessary to choose a perturbation consistent with the initial conditions. This is discussed below.

We consider the coordinate system in which the disturbance is at rest. The problem is then one of steady flow over a wavy wall of small amplitude ε. The solution to this problem is well known for a medium of infinite extent(11). If the interface wave is described by

$$y = \varepsilon \text{ Sin } \alpha x$$

it is easily shown that the perturbed velocity is

$$\delta Vx = - \frac{U\varepsilon}{\sqrt{1 - M^2}} \exp \left(- \alpha \sqrt{1 - M^2}\, y\right) \text{ Sin } \alpha x$$

$$\delta Vy = U\varepsilon\alpha \exp \left(- \alpha \sqrt{1 - M^2}\, y\right) \text{ Cos } \alpha x$$

where M is the Mach number of the unperturbed flow ($M^2 << 1$); the perturbed pressure is

$$\delta p = - \rho\, \delta\, V_x\, U$$

and the perturbed density is obtained from an equation of state. This model is also adequate when the y-boundaries are fixed since the attenuation of the perturbation in the y-direction is $\sim e^{-\pi}$ even for the longest wavelength.

A numerical calculation for the m = 2 mode showed that the interface was indeed unstable to a small perturbation. However quantitative measurements of the growth rates using MODANA were not consistent with linear theory. This discrepancy is not yet understood and will be investigated further. Figure 11 shows a series of plots of the interface nodes at various times during the evolution of the instability.

(b) Supersonic flow

The case of supersonic flow relative to the interface has been treated analytically only for a medium of infinite extent. In this case it can be shown(9) that if the Mach number exceeds some critical value ($\sqrt{2}$ for a perfect gas) then the flow is stable. In the case of supersonic flow, however, there is no attenuation of the perturbation. Instead, the same value of the perturbation exists along straight lines inclined at the Mach angle with respect to the undisturbed flow. Thus, the situation is complicated by the presence of fixed y-boundaries when reflections and resonances can be expected. However, if we consider the steady supersonic flow in a tube of varying cross-section we find from the continuity and momentum equations that

$$\frac{dp}{p} = - \frac{dA}{A}$$

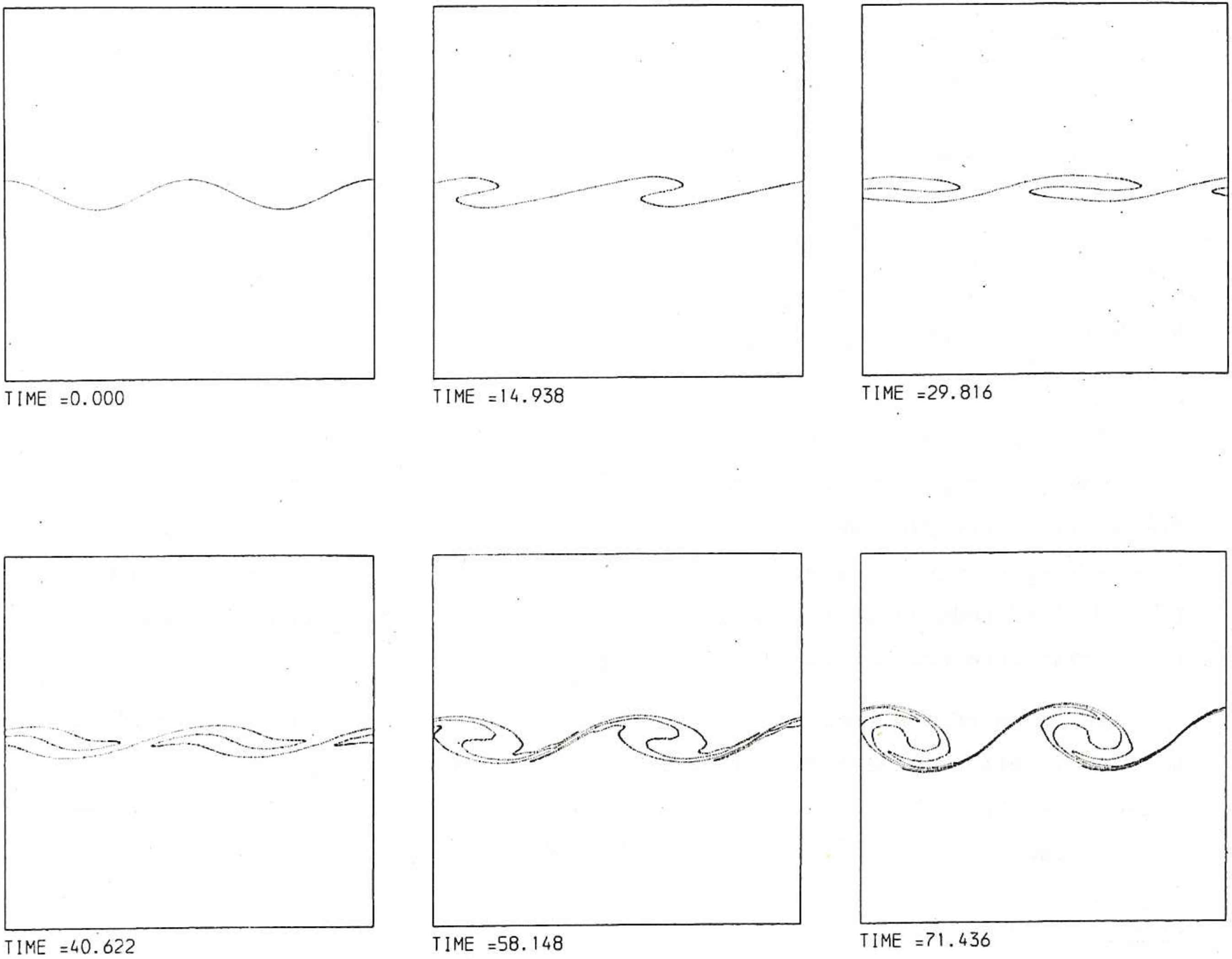

TIME =0.000

TIME =14.938

TIME =29.816

TIME =40.622

TIME =58.148

TIME =71.436

Fig. 11 Evolution of the Kelvin-Helmholtz instability (Mach No. = 0.5)

CR 72 113

where p is the pressure and A is the cross-sectional area of the channel. One therefore expects a tendency to stabilize any small perturbation of the interface.

A numerical calculation was carried out with a steady state Mach number of 1.5. During the time of the calculation there was no discernable growth of an initial perturbation. The growth rate compared with the subsonic case was therefore at least an order of magnitude less.

7. FUTURE APPLICATIONS

This report has described the HYDRA model to study the flow of compressible media with a deformable interface between them. Under some circumstances there can be more than two substances present. The problems outlined below are planned or are currently being studied to elucidate various features of liquid metal-water interactions.

High speed movie-films of molten metal dropped into water highlight the importance of vapour bubbles in triggering explosive processes. Therefore, calculations are planned to (1) study the stability of vortex sheets generated by shock waves when they encounter density discontinuities and (2) to study the jetting produced by collapsing bubbles in asymmetric situations which could penetrate the hot metal and lead to shredding.

A second area of work is to simulate the dynamics of the Q* experiment. A first simple calculation, for which experimental data are available, will simulate the growth of a N_2 bubble in water with a N_2 gas blanket above the free surface.

ACKNOWLEDGEMENTS

I wish to thank Dr K V Roberts for his active interest at all stages of this work and Mr J P Christiansen for many helpful discussions during development of the code.

References:

1. BERK, H L, and ROBERTS, K V, "Methods in Computational Physics", Academic Press, 1970.

2. RICHTMYER, R D and MORTON, K W, "Difference Methods for Initial-Value Problems", Wiley (Interscience), New York, 1967.

3. MORTON, K W, Proc. Computational Physics Conference, VOL. 1, Culham, 1969.

4. LAPIDUS, A, Journal of Computational Physics 2, 154-177, 1967.

5. RUBIN, E L and BURSTEIN, S Z, Journal of Computational Physics, 2, 178-196, 1967.

6. AMSDEN, A A, Los Alamos Report, LA 3466. "Particle in Cell Method for the Calculation of the Dynamics of Compressible Fluids", 1966.

7. ROBERTS, K V and CHRISTIANSEN, J P, to be published

8. GERWIN, R A, Rev. Mod. Phys., vol. 40, No. 3, 652-658, 1968.

9. MILES, J W, J. Fluid Mech. 4, 538-552, 1958.

10. PLESSET, M S, and HSIEH, D Y, Phys. Fluids 7, 1099, 1964.

11. LIEPMANN, H, and ROSHKO, A "Elements of Gas Dynamics" Wiley and Sons, New York, 1957, Chapt. 8.

12. ROBERTS, K V, Fast Reactor Safety Note, FRSN 3/74.